Available online at www.sciencedirect.com

ScienceDirect

Procedia Structural Integrity 3 (2017) 468–476

Structural Integrity Procedia

www.elsevier.com/locate/procedia

XXIV Italian Group of Fracture Conference, 1-3 March 2017, Urbino, Italy

On the fracture processes of cutting

P. Ståhle[a], A. Spagnoli[b,*], M. Terzano[b]

[a]*Division of Solid Mechanics, Lund University, SE-221 00 Lund, Sweden*
[b]*Department of Engineering and Architecture, University of Parma, Viale Usberti 181/A, 43124 Parma, Italy*

Abstract

The process of cutting is treated as a fracture mechanical process. For an elliptic rigid wedge pressed into an elastic material, fracture may occur as an autonomous process if the tip of the wedge is sufficiently blunt or is affected by the geometry of the wedge if the tip is sharp. The conditions leading to the former or the latter case is obtained as a relation between the wedge tip radius, the fracture toughness and the modulus of elasticity. These limits and the intermediate states are discussed. The implications of the drastic changes of the mechanical state of the near tip region when the wedge edge is sharp are also discussed.

Keywords: Cutting; fracture processes; linear elastic; fracture toughness.

1. Introduction

The mechanics of cutting has been attracting much attention in the literature, with the aim of addressing different technical problems (Williams and Patel, 2016; Williams et al., 2016) ranging from metal machining (Williams, 1998; Williams et al., 2010), to cutting of soft solids, such as biological tissues, foodstuffs or elastomeric materials (Goh et al., 2005; McCarthy et al., 2007, 2010). Cutting is also used as an experimental method for determining fracture toughness of polymers (Patel et al., 2009). Typically, cutting process is characterized by an indentation stage followed by a stage where the target material undergoes a progressive separation. The mechanical response in both stages is governed by the cutting tool shape (blade), the target material and the cutting rate. In the present paper, the quasi-static fracture stage is studied by means of a simple model which can be handled analytically, where the blade is modelled as a rigid wedge inserted into an elastic plate.

2. The wedge model for the cutting tool

Let us consider a large plate with a single centred cut of length $2a$. A cartesian coordinate system x, y is introduced in the centre of the plate so that the cut covers the region $|x| \leq a$, $y = 0$. An elliptic wedge with major and minor

* Corresponding author. Tel.: +39-0521-905927 ; fax: +39-0521-905924.
E-mail address: spagnoli@unipr.it

10.1016/j.prostr.2017.04.063

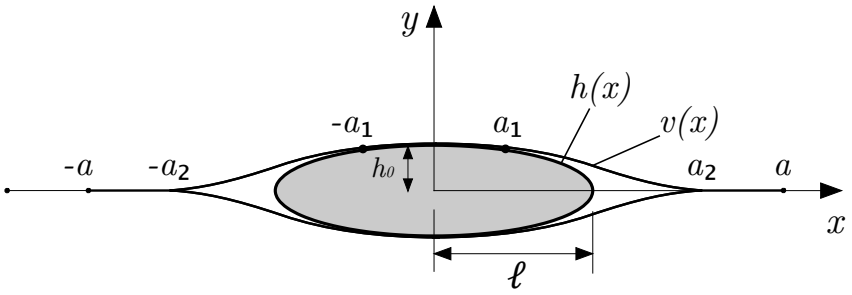

Fig. 1. An elliptic rigid wedge $|x|\leq\ell$ is inserted in a straight cut $|x|\leq a$, in a very large elastic plate. The wedge imposes a known displacement $h(x)$ in the region $|x|\leq a_1$ and traction free surfaces in the regions $a_1<|x|<a_2\leq a$, where contact between the cut surfaces is lost. Displacements vanish in $a_2 \leq |x| \leq a$.

semiaxes of length, respectively, ℓ and h_0, is inserted in the centre of the crack (Fig. 1). Its shape is expressed by

$$h(x) = h_o \sqrt{1 - (x/\ell)^2} \tag{1}$$

In order to define the wedge sharpness, we introduce the radius of curvature ρ at the wedge tip, which is equal to h_o^2/ℓ. A sharpness parameter θ can be defined if one divides ρ by a material-based length parameter. In absence of any inherent material length, the tip radius R_c of a crack experiencing a critical condition is considered, defined as

$$R_c = \left(\frac{\pi}{2}\right)\left(\frac{K_{\mathrm{I}c}}{E}\right)^2 \tag{2}$$

where $K_{\mathrm{I}c}$ is the critical stess intensity factor and E is Young's modulus. Therefore we obtain

$$\theta = \frac{h_0^2}{\ell R_c} \tag{3}$$

The wedge is assumed to be sharp for $\theta < 1$ and blunt for $\theta > 1$.

We assume the wedge to be shorter or have the same length of the cut, i.e., $\ell \leq a$ and partly in contact with its surfaces, which are supposed to be friction free. The elastic plate is assumed to be stress free far away from the wedge. As a result of the contact between the wedge and the cut surfaces, normal tractions can only be compressive or absent, i.e., $\sigma_y \leq 0$, along $|x| \leq a_1$, while shear tractions $\tau_{xy}(x)$ are null at all points along $y = 0$ because of frictionless surfaces. Moreover, the wedge generates imposed displacements $v(x) = h(x)$ in $|x| \leq \ell$.

In view of this, a boundary value problem can be formulated. Considering the upper half of the plate, such a problem is defined by the following equations

$$v(x) = h(x), \quad \text{with the condition} \quad \sigma_y(x) \leq 0 \quad \text{for} \quad |x| \leq a_1 \tag{4}$$

In the open part of the cut we have

$$\sigma_y(x) = 0 \quad \text{for} \quad a_1 \le |x| \le a_2\,, \tag{5}$$

with the conditions that

$$v(x) > \begin{cases} h(x) & \text{for} \quad a_1 < |x| < \ell \\ 0 & \text{for} \quad \ell \le |x| < a_2 \end{cases} \tag{6}$$

In the closed part of the cut the symmetry across $y = 0$ implies that

$$v(x) = 0, \quad \text{with the condition} \quad \sigma_y(x) \le 0 \quad \text{for} \quad a_2 \le |x| < a \tag{7}$$

Ahead of the cut, continuity and symmetry bring the displacements unconditionally to zero

$$v(x) = 0 \quad \text{for} \quad |x| \ge a \tag{8}$$

while no conditions regarding permissible normal tractions can be established, which therefore may be tensile and possess stress singularities. Finally, shear stresses vanish everywhere along the crack plane

$$\tau_{xy}(x) = 0 \quad \text{for} \quad y = 0 \tag{9}$$

3. The fracture mechanics analysis of the cutting process

The problem given by the boundary conditions (1) to (9) is decomposed into two different cases. The first case has a known solution while the second is solved below. A superposition will provide us with the solution of the overall problem.

3.1. Case 1

As mentioned earlier, a closely related problem is that of a plate with a crack subjected to a uniform pressure, σ_o, applied to the crack surfaces, see Fig. 2. Considering a crack length of 2ℓ, the vertical displacement of the upper crack surface becomes (Broberg, 1999)

$$v(x) = \frac{2\sigma_o}{E}\sqrt{\ell^2 - x^2} \quad \text{for} \quad |x| \le \ell \tag{10}$$

Plane stress conditions are assumed. For plane strain, the modulus of elasticity E is replaced with $E/(1-\nu^2)$, where ν is Poisson's ratio. The normal stress in the y-direction along the rest of the crack plane is

$$\sigma_y(x) = \sigma_o\left(\frac{x}{\sqrt{x^2 - \ell^2}} - 1\right) \quad \text{for} \quad |x| > \ell \tag{11}$$

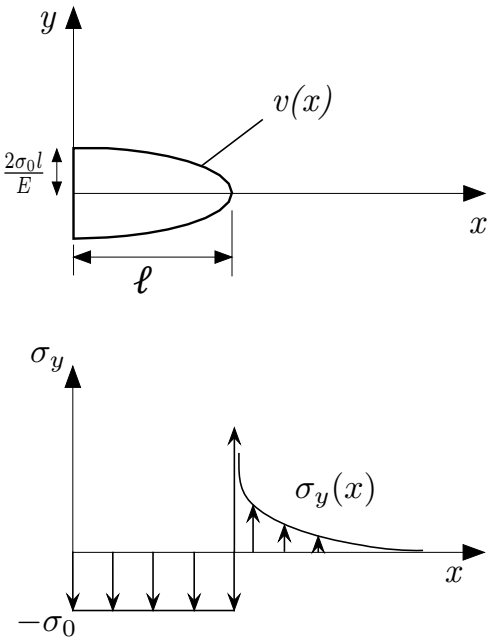

Fig. 2. Case 1 is here illustrated. The sketch shows the equivalence with a crack of length 2ℓ, with a uniform pressure σ_o applied to its surfaces. According to (10), displacements in $|x| \le \ell$ are $v(x) = h(x)$ if the crack is subjected to the surface pressure given by (12).

As it is readily seen, (10) constitutes an ellipse whose mathematical description has the same form of the wedge shape, equation (1). Equivalence is obtained if

$$\sigma_o = \frac{Eh_o}{2\ell} \tag{12}$$

The stress intensity factor K_R for both crack tips, using (12), is given by

$$K_R = \sigma_o \sqrt{\pi\ell} = \frac{Eh_o}{2}\sqrt{\frac{\pi}{\ell}} \tag{13}$$

A detailed solution can be found in Tada et al. (1985).

3.2. Case 2

The second case considers a crack that occupies the open part of the cut, i.e., $a_1 \le |x| < a_2$. In order to equilibrate the normal stresses of Case 1, as (5) requires, the following tractions need to be applied to the crack surfaces (Fig.3a)

$$\sigma_y(x) = \begin{cases} \sigma_o \quad \text{for} \quad a_1 \le |x| < \ell \\ \sigma_o\,(1 - \frac{x}{\sqrt{x^2-\ell^2}}) \quad \text{for} \quad \ell \le |x| < a_2 \end{cases} \tag{14}$$

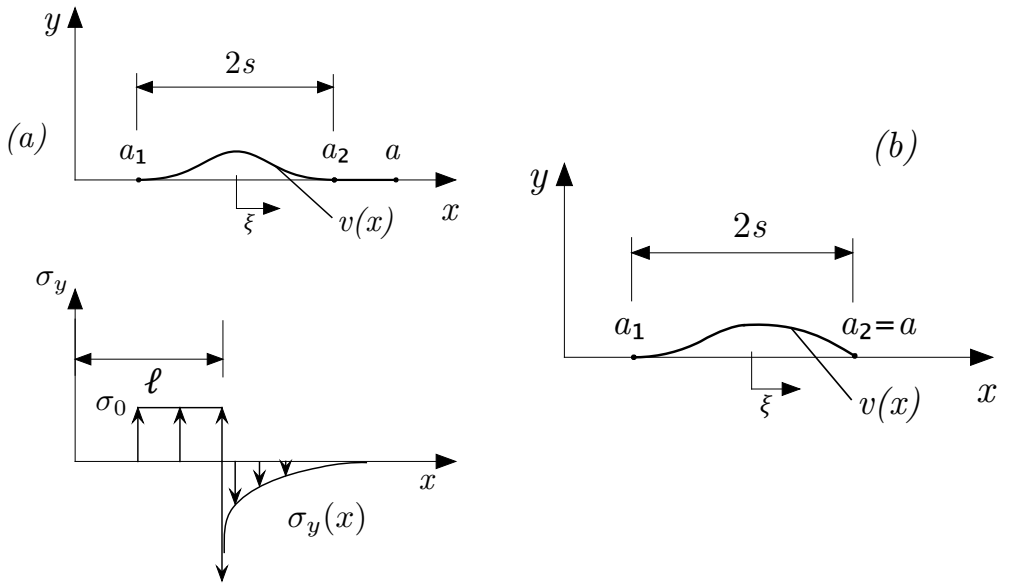

Fig. 3. Case 2 is here illustrated. Because of the symmetry, only a quarter of the plate is considered. *(a)* The displacements $v(x)$ are caused by the removing of the tractions that are present between a_1 and a_2 in Case 1. Since a_2 is a contact point, tractions in $a_2 \leq |x| < a$ cannot be tensile. *(b)* The special case of $a_2 = a$ is considered, which allows singular tensile stresses, giving rise to a discontinuity in displacements derivative at $x = a_2 = a$.

Displacements in the remaining parts of the crack plane are as follows

$$v(x) = 0 \quad \text{for} \quad |x| > a_2 \quad \text{and for} \quad |x| < a_1 \tag{15}$$

The problem given by the boundary conditions (14) and (15) generally possesses stress singularities at $|x| = a_1$ and at $|x| = a_2$. These are defined by their respective stress intensity factors K_{I,a_1} and K_{I,a_2}. The contact conditions, that do not allow neither transmission of tensile stresses, equation (4) nor overlapping of surfaces, equation (6), exclude negative and positive stress intensity factors for both extremes, therefore leaving

$$K_{\mathrm{I},a_1} = K_{\mathrm{I},a_2} = 0 \quad \text{for } a_2 \leq a \tag{16}$$

We can use the previous conditions to determine the position of a_1 and a_2. Possibly, when the cut is short, the wedge will at some point, while moving in either positive or negative x-direction, cause a_2 to reach a, implying the situation which is illustrated in Fig.3b. In this case, the position of a_2 is known and therefore (16) is replaced by the following

$$K_{\mathrm{I},a_1} = 0, \qquad K_{\mathrm{I},a_2} \geq 0 \quad \text{for } a_2 = a \tag{17}$$

In order to find the expression of the stress intensity factors, we limit our analysis to cases for which $a_2 - a_1 \ll \ell$, which allows us to ignore the changes that are caused by the applied stresses in the opposite region, i.e., for $-a_2 < x < -a_1$, thus simplifying considerably the analysis. Solution is obtained using known weight functions, by which the

stress intensity factors are obtained as follows

$$K_{\mathrm{I}} = -\frac{1}{\sqrt{\pi s}} \int_{-s}^{s} \sigma_y(\xi) \sqrt{\frac{s+m\xi}{s-m\xi}} \mathrm{d}\xi \tag{18}$$

where $s = (a_2 - a_1)/2$, $x = \xi + (a_1 + a_2)/2$, $m = -1$ for crack tip at $x = a_1$ and $m = 1$ for crack tip at $x = a_2$. Replacing $\sigma_y(x)$ from (14), the previous integral is conveniently split into two parts

$$K_{\mathrm{I},n} = K_{\mathrm{I},n}^{(1)} + K_{\mathrm{I},n}^{(2)} \tag{19}$$

where n equals a_1 or a_2. With $t = \ell - (a_1 + a_2)/2$ and $k(m,\xi) = \sqrt{\frac{s+m\xi}{s-m\xi}}$, stress intensity factors are

$$K_{\mathrm{I},n}^{(1)} = -\frac{\sigma_o}{\sqrt{\pi s}} \int_{-s}^{t} k(m,\xi)\mathrm{d}\xi = -\sigma_o \sqrt{\pi s} \tag{20}$$

$$K_{\mathrm{I},n}^{(2)} = \frac{\sigma_o}{\sqrt{\pi s}} \int_{t}^{s} \frac{\ell - t + \xi}{\sqrt{(\xi - t)(2\ell - t + \xi)}} k(m,\xi)\mathrm{d}\xi \tag{21}$$

By applying the transformation $u = \xi/s$, $\hat{t} = t/s$ and $\hat{\ell} = \ell/s$ to (20) and (21), we obtain

$$K_{\mathrm{I},n} = -\sigma_o \sqrt{\pi} + \frac{\sigma_o}{\sqrt{\pi}} \int_{\hat{t}}^{1} \frac{\hat{\ell} + u - \hat{t}}{\sqrt{(u - \hat{t})(2\hat{\ell} + u - \hat{t})}} k(m,u)\mathrm{d}u \tag{22}$$

and using condition (16), we obtain the following expression, for $n = a_1$

$$K_{\mathrm{I},a_1} = K_{\mathrm{I},a_1}^{(1)} + K_{\mathrm{I},a_1}^{(2)} = 0 \quad \Rightarrow \quad \int_{\hat{t}}^{1} \frac{\hat{\ell} + u - \hat{t}}{\sqrt{(u - \hat{t})(2\hat{\ell} + u - \hat{t})}} \sqrt{\frac{1-u}{1+u}} \mathrm{d}u = \pi \tag{23}$$

Equation (23) provides a relation between a_1 and a_2 for any given $\hat{\ell}$, and it can be rewritten with the following recursion which yields a single root $d_i = 1/\hat{\ell} = s/\ell$

$$d_i = \left(\frac{1}{\pi} \int_{\hat{t}}^{1} \frac{1 + (u - \hat{t}) d_{i-1}}{\left(\sqrt{(u - \hat{t})(2 + (u - \hat{t}) d_{i-1}} \right)} \sqrt{\frac{1-u}{1+u}} \mathrm{d}u \right)^2, \quad \text{with} \quad d_0 = 0 \tag{24}$$

The recursion cycles are assumed to proceed until a converged result is obtained after N cycles. The obtained value d_N is denoted d. The stress intensity factor at $x = a_2$ is given by

$$K_{\mathrm{I},a_2} = K^{(1)}_{\mathrm{I},a_2} + K^{(2)}_{\mathrm{I},a_2} = \sigma_o \sqrt{\pi}\left(\frac{1}{\pi}\int_{\hat{t}}^{1} \frac{\hat{\ell} + (u-\hat{t})}{\sqrt{(u-\hat{t})(2\hat{\ell}+u-\hat{t})}}\sqrt{\frac{1+u}{1-u}}\mathrm{d}u - 1\right) \tag{25}$$

Normalizing with K_R, from (13), the dimensionless stress intensity factor is

$$\frac{K_{\mathrm{I},a_2}}{K_R} = \frac{1}{\pi}\int_{\hat{t}}^{1} \frac{1 + (u-\hat{t})d}{\sqrt{(u-\hat{t})(2+(u-\hat{t})d)}}\sqrt{\frac{1+u}{1-u}}\mathrm{d}u - \sqrt{d} \tag{26}$$

3.3. A wedge with a parabolic shape

Equation (1) can be written as

$$h(x) = h_o\sqrt{2 - \frac{\ell - x}{\ell}}\sqrt{\frac{\ell - x}{\ell}} \tag{27}$$

Accordingly, it can be noticed that near the wedge tip, i.e. for $(\ell - x)/\ell \to 0$, the ellipse degenerates to a parabola (Fig. 4), namely

$$h(x) = h_o\sqrt{\frac{2}{\ell}}\sqrt{\ell - x}$$

thus, equation (24) for a parabolic wedge is rewritten as

$$d = \frac{1}{4\pi^2}\left(\int_{\hat{t}}^{1}\sqrt{\frac{1-u}{u-\hat{t}}}\mathrm{d}u\right)^2 \tag{28}$$

with the limit solution $\hat{t} \to 1$ as $d \to 0$. The stress intensity factor K_{I,a_2} is obtained as the limit for $\ell \to \infty$ in equation (25), and in dimensionless form is

$$\frac{K_{\mathrm{I},a_2}}{K_R} = \frac{1}{\pi}\int_{\hat{t}}^{1}\frac{\mathrm{d}u}{\sqrt{(u-\hat{t})(1-u)}} \tag{29}$$

However, the contact conditions require that (23) is fulfilled for both the elliptic and parabolic wedge.

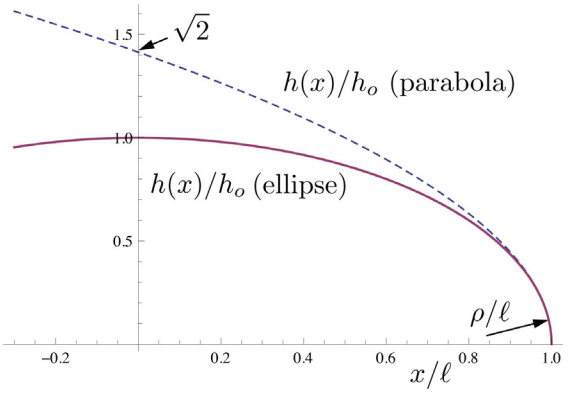

Fig. 4. Comparison of elliptic and parabolic wedges, having the same radius of curvature ρ at their tip.

4. Results and concluding remarks

The recursion (24) is used to determine the positions of a_1 and a_2 in the elliptic wedge. For the parabolic wedge, the wedge length ℓ does not affect the mechanical state in the end region close to the wedge tip. The ratio $d = s/\ell$ is obtained as an exact result, thanks to the simplifications that can be introduced in the expression of d, equation (28). Once d is known, the stress intensity factor at the foremost end $x = a_2$ of the open region is calculated through (26) and (29) for the elliptic and parabolic wedges, respectively.

Let us consider an initial crack of semi-length a_o and two different scenarios of a blunt wedge, $\theta > 1$, and of a sharp wedge, $\theta < 1$. As noted in §2, the definition of wedge sharpness depends on the wedge tip radius ρ and on the target material through R_c, equation (2). The solution for the stress intensity factor K_{I,a_2}, both in the case of an elliptic and parabolic wedge, is obtained and the results are summarized in Fig. 5. The stress intensity factor at the crack tip is shown as a function of a dimensionless distance between the wedge tip and the initial crack tip. The values of K_{I,a_2} are normalized with respect to the stress intensity factor K_R that would develop if the wedge fills the entire crack with no gap, as obtained in §3.1. Using the definition of the wedge tip radius ρ in (13) we obtain

$$K_R = E\sqrt{\pi\rho/2} \tag{30}$$

We may note that, when $(\ell - a_o) <\approx -0.9\ell$ for an elliptic wedge and $\ell - a_o <\approx -0.8\ell$ for a parabolic wedge, $a_2 < a_o$, that is, the initial crack is partially closed, no stress singularity occurs and $K_{\mathrm{I},a_2} = 0$. For relatively greater values of $(\ell - a_o)$, $a_2 = a_o$ and $K_{\mathrm{I},a_2} > 0$.

If one immagines to push the wedge, e.g. rightwards, the distance $(a_o - \ell)$ decreases and K_{I,a_2} increases. Different series of events will take place depending on the wedge sharpness. If the wedge is blunt ($\theta > 1$), K_{I,a_2} increases with decreasing $(a_o - \ell)$ until it reaches the critical stress intensity factor $K_{\mathrm{I},c}$. At this point, the crack propagates in a stable manner, so that the distance between the current crack tip and the wedge tip $(a - \ell)$ remains constant, while obviously $(a_o - \ell)$ decreases. In other words, when the wedge is pushed ahead, it will never reach the crack tip. On the other hand, if the wedge is sharp ($\theta < 1$), K_{I,a_2} increases with decreasing $(a_o - \ell)$ as before but eventually the wedge tip will reach the initial crack tip, i.e., $\ell = a_0$, and the stress intensity factor K_{I,a_2}, attaining the value K_R, is still less than the material toughness $K_{\mathrm{I},c}$. The force that has to be applied to the wedge to propagate the initial crack, if we suppose the fracture processes not affected by the compressive stresses caused by the wedge, is obtained as

$$F = \frac{\left(K_{\mathrm{I}c}^2 - K_R^2\right) b}{E} \tag{31}$$

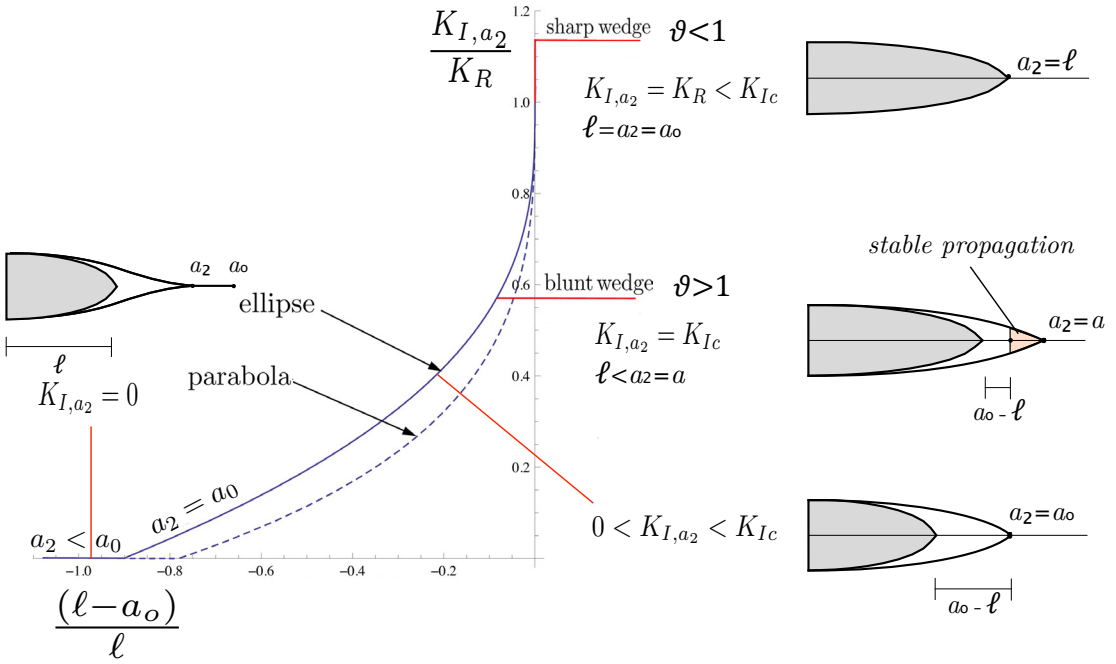

Fig. 5. Dimensionless stress intensity factor $K_{I,a_2}/K_R$ as a function of the normalized distance between the wedge tip and the initial crack tip $(\ell - a_o)/\ell$. The results for a blunt wedge ($\theta > 1$) and for a sharp wedge ($\theta < 1$) are reported.

where b is the plate thickness.

Acknowledgements

The first two authors gratefully acknowledge the financial support for staff mobility within the framework of Erasmus+ project.

References

Broberg, K. B., 1999. Cracks and fracture. Academic Press.

Goh, S., Charalambides, M., Williams, J., 2005. On the mechanics of wire cutting of cheese. Engineering fracture mechanics 72 (6), 931–946.

McCarthy, C. T., Annaidh, A. N., Gilchrist, M. D., 2010. On the sharpness of straight edge blades in cutting soft solids: Part ii–analysis of blade geometry. Engineering Fracture Mechanics 77 (3), 437–451.

McCarthy, C. T., Hussey, M., Gilchrist, M. D., 2007. On the sharpness of straight edge blades in cutting soft solids: Part i–indentation experiments. Engineering Fracture Mechanics 74 (14), 2205–2224.

Patel, Y., Blackman, B., Williams, J., 2009. Determining fracture toughness from cutting tests on polymers. Engineering Fracture Mechanics 76 (18), 2711–2730.

Tada, H., Paris, P., Irwin, G., 1985. The stress analysis of crack handbook, del research, st. Louis, MO.

Williams, J., 1998. Friction and plasticity effects in wedge splitting and cutting fracture tests. Journal of Materials science 33 (22), 5351–5357.

Williams, J., Atkins, A., Charalambides, M., Lucas, P., 2016. Cutting science in biology and engineering.

Williams, J., Patel, Y., 2016. Fundamentals of cutting. Interface focus 6 (3), 20150108.

Williams, J., Patel, Y., Blackman, B., 2010. A fracture mechanics analysis of cutting and machining. Engineering Fracture Mechanics 77 (2), 293–308.